Metamagnetic domains in antiferromagnetically coupled multilayers with perpendicular anisotropy

N. S. Kiselev,[1,2,*] C. Bran,[1] U. Wolff,[1] L. Schultz,[1] A. N. Bogdanov,[1] O. Hellwig,[3] V. Neu,[1] and U. K. Rößler[1,†]

[1]*IFW Dresden, Postfach 270116, D-01171 Dresden, Germany*

[2]*Donetsk Institute for Physics and Technology, 83114 Donetsk, Ukraine*

[3]*San Jose Research Center, Hitachi Global Storage Technologies, San Jose, California 95135, USA*

(Received 14 August 2009; revised manuscript received 17 November 2009; published 5 February 2010)

In antiferromagnetically coupled superlattices with perpendicular anisotropy an applied magnetic-bias field stabilizes specific multidomain states, so-called *metamagnetic* domains. A phenomenological theory developed in this paper allows to derive the equilibrium sizes of metamagnetic stripe and bubble domains as functions of the antiferromagnetic exchange, the magnetic-bias field, and the geometrical parameters of the multilayer. The magnetic-phase diagram includes three different types of metamagnetic domain states, namely, multidomains in the surface layer and in internal layers, also mixed multidomain states may arise. Experimental investigations have been carried out for a [Co/Pt]/Ru superlattice consisting of $N=18$ antiferromagnetically coupled ferromagnetic blocks with $X=7,8,9$ Co/Pt bilayers, each, and in another system with $N=10$ and $X=5$. Magnetization curves and magnetic-force-microscopy images for [Co/Pt]/Ru superlattices provide detailed information on the magnetization reversal during the metamagnetic reorientation.

DOI: 10.1103/PhysRevB.81.054409 PACS number(s): 77.80.Dj, 75.70.Cn, 75.70.Kw, 68.37.Rt

I. INTRODUCTION

Ferromagnetic (FM) multilayers with antiferromagnetic (AF) interlayer coupling are widely used in spin valves and various other spin-electronics devices, and they are considered as promising materials for thermally stable high-density recording technologies.[1] On the other hand, such high-quality multilayer stacks represent "artificial" nanoscale antiferromagnets and provide ideal experimental models to investigate general magnetic phenomena including physical properties of confined magnetic systems influenced by surface effects.[2] For example, recently experimental[3] and theoretical[4] investigations of antiferromagnetically coupled [Fe/Cr] multilayers have resolved the long-standing problem of "surface spin flop" in uniaxial antiferromagnets.[5] Recently synthesized antiferromagnetically coupled multilayers with strong perpendicular anisotropy ([Co/Pt]/Ru, [Co/Pt]/Ir and others) represent a novel and intensively investigated class of artificial antiferromagnetic nanostructures.[6] In these systems strong competition between short-range interlayer exchange coupling and long-range dipolar interactions results in a rich variety of magnetization-reversal processes accompanied by unusual reorientation transitions and the formation of complex multidomain structures.[6–13]

Depending on the values of magnetic and geometrical parameters experimentally investigated multilayers[6,14] have either (i) single-domain antiferromagnetic or (ii) ferromagnetic multidomain ground states.[15] The AF single-domain phase is favored by the exchange coupling and is observed in multilayers with relatively thin ferromagnetic blocks while FM stripes are stabilized in systems with thicker ferromagnetic blocks. In Refs. 6 and 14 the ground state of [Co/Pt]/Ru multilayers has been altered by variation in the Co layers thicknesses or by changing the number of Co/Pt bilayers in the ferromagnetic blocks.

Magnetization processes in [Co/Pt]/Ru multilayers strongly depend on the type of the ground state. In an applied magnetic field the FM stripe phase evolves similarly to common stripes in ferromagnetic layers.[16] Detailed experimental and theoretical investigations of multidomain states and magnetization processes in [Co/Pt]/Ru multilayers with FM stripe ground state have been carried out in our recent work.[17] In the present paper we now study [Co/Pt]/Ru multilayers with the AF single-domain ground state. In this case, AF phases transform into the saturated state via a first-order transition accompanied by the formation of multidomain states.[6,13] In some basic physical aspects the multilayers in the AF ground state are similar to bulk antiferromagnets with strong uniaxial anisotropy (so-called, *metamagnets*)[18] and, thus, can be classified as *synthetic metamagnets*.[13,19] In particular, characteristic magnetic-field-induced domains have been observed in [Co/Pt]/Ru (Refs. 6 and 7) and [Co/Pd]/Ru (Ref. 10) superlattices. They are analogous to *metamagnetic domains* which have been observed in many bulk metamagnets.[20]

The close physical resemblance between the metamagnetic domains and common ferromagnetic stripes in multilayers has been clearly demonstrated in various experiments on perpendicular multilayers, Ref. 6. For example, it was shown that the magnetization curve of an antiferromagnetic $\{[\mathrm{Co}(4\ \text{Å})/\mathrm{Pt}(7\ \text{Å})]_4/\mathrm{Co}(4\ \text{Å})/\mathrm{Ru}(9\ \text{Å})\}_{10}$ multilayer in the region of a bulk metamagnetic transition is similar to the magnetization curve of a pure ferromagnetic $\{[\mathrm{Co}(4\ \text{Å})/\mathrm{Pt}(7\ \text{Å})]_5\mathrm{Co}(4\ \text{Å})/\mathrm{Pt}(57\ \text{Å})\}_5$ multilayer. For more detail, see Ref. 6, Fig. 30. Here, we investigate the magnetic-field-driven evolution of the metamagnetic domains, both theoretically and by experiment. The comparison of theoretical calculations for the anhysteretic magnetization process and the possible magnetic equilibrium-phase sequences allows to understand the experimentally observed magnetization processes in [Co/Pt]/Ru superlattices with AF single-domain ground state.

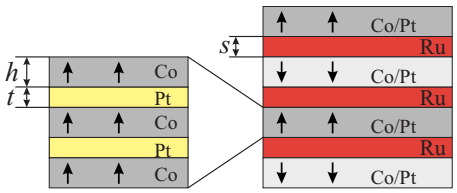

FIG. 1. (Color online) Sketch of an antiferromagnetically coupled multilayer consisting of $\{[\mathrm{Co}(h)/\mathrm{Pt}(t)]_{X-1}/\mathrm{Co}(h)/\mathrm{Ru}(s)\}_N$ with $X=3$ and $N=4$.

II. MODEL AND THEORETICAL ANALYSIS

As a basic model for $\{[\mathrm{Co}/\mathrm{Pt}]_{X-1}/\mathrm{Co}/\mathrm{Ru}\}_N$ superlattices we consider N identical "ferromagnetic blocks" composed of X bilayers $[\mathrm{Co}(h)/\mathrm{Pt}(t)]$, antiferromagnetically coupled via $N-1$ Ru(s) spacers (where h, t, and s are the thicknesses of the corresponding nanolayers, Fig. 1). In this contribution we consider the cases with an even number of N only. Due to their net magnetization multilayers with an odd number of N can be considered as *artificial ferrimagnets*. These systems are markedly different from the antiferromagnetic systems discussed here. The properties of such ferrimagnetic multilayers, even at zero field are mainly determined by their noncompensated total magnetization. They will be considered elsewhere.

We assume that the perpendicular uniaxial anisotropy originating from the Co interface anisotropy is strong enough to stabilize the perpendicular orientation of the magnetization **M** in magnetic domains (Fig. 2). In the antiferromagnetic single-domain phase a sufficiently strong magnetic field applied perpendicular to the multilayer surface (a *bias* field) "overturns" the antiparallel magnetization (Fig. 2).

The reorientation field for a certain ferromagnetic block depends on the strength of the antiferromagnetic interaction with adjacent blocks. For a multilayer consisting of identical blocks, antiferromagnetic coupling of the interior blocks is two times stronger than that of the two outmost layers. Correspondingly field-driven reorientations may occur as a two-step process: the surface block having its magnetization oriented against the applied field switches before the remaining interior blocks reorient. Both processes in the surface layer and in the bulk of the multilayer stack usually proceed gradually by redistribution of stripe domains with antiparallel orientation. In the following these domain states are referred to as *metadomains* or *metamagnetic domains*. Due to long-range magnetostatic interactions the walls of the bulk metamagnetic domains sit exactly on top of each other in ferromagnetic layers throughout the whole stack, Fig. 2. Furthermore, in the infinite layer approximation homogeneously magnetized ferromagnetic blocks do not interact with other blocks due to the localization of their stray fields within the layers. Thus, such metamagnetic domains are described by the regular model of a two-phase domain structure in a ferromagnetic multilayer consisting of X equidistant ferromagnetic monolayers that form one ferroblock (Fig. 2). In the case of the metadomains in the bulk of the multilayer stack, the spacers have different thicknesses, t within blocks and $L=2s+L_b$ $[L_b=Xh+(X-1)t]$ between ferroblocks [Fig. 2(b)].

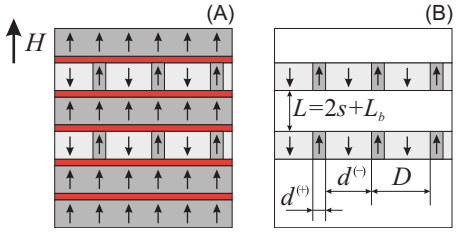

FIG. 2. (Color online) (a) Multilayer ($N=6$) where the surface layer has already switched and metamagnetic stripes are formed in the interior. (b) The layers are equivalent to stripes in two ferromagnetic blocks separated by distance $L=2s+L_b$, where $L_b=Xh+(X-1)t$ is the ferroblock thickness.

The energy density of the metamagnetic stripes (per one magnetic layer) in an applied magnetic bias field H (Ref. 13)

$$w = w_w + w_{ex} + w_m - HM_s(d_+ - d_-)/D \tag{1}$$

includes the domain-wall energy $w_w=2\sigma/D$ (where σ is the area energy density, $D=(d_++d_-)$ is the stripe period, and $d_\pm$ are the domain sizes, Fig. 2); the interlayer exchange energy w_{ex}, stray-field energy w_m, and Zeeman energy. Note that for metamagnetic domains the exchange coupling is proportional to the difference between domain sizes, $w_{ex}\propto(d_+-d_-)$ (Fig. 2). This means that the interlayer exchange acts as a certain applied field. Introducing an effective *exchange-bias* field

$$H_{ex} = \alpha J/(hXM_s) \tag{2}$$

allows to include it into the Zeeman term. Here J is the strength of the antiferromagnetic interlayer coupling, and the factor $\alpha=1$ or 2 has to be used for surface and internal metamagnetic domains, respectively. After that, the energy density w from Eq. (1) can be reduced to the following form:

$$w = 8\pi M_s^2 \frac{l_c}{D} - \mathcal{H}M_s q + 2\pi M_s^2 \mathcal{N}, \tag{3}$$

where $\mathcal{H}=(H-H_{ex})$ is an effective magnetic field, $l_c=\sigma/(4\pi M_s^2)$ is the *characteristic* length, $q=(d_+-d_-)/D$ equals the reduced magnetization of the stripe phase, and the effective demagnetizing factor $\mathcal{N}=\mathcal{N}(D,q)$ describes the stray-field energy of the stripes and is a function of the variables D and q. The energy density in Eq. (3) functionally coincides with that for a ferromagnetic multilayer in the applied field $\mathcal{H}$. This reduces the problem to a model for common ferromagnetic domains in multilayers with spacers of thicknesses $L=2s+L_b$ in an "applied magnetic field" $\mathcal{H}$ (Fig. 2).

Due to the mathematical identity of electrostatic and magnetostatic equations[16] the multilayer with stripes can be thought as a set of planes with "charged" stripes, and the stray-field energy includes contributions from interactions of all these layers. For two "striped" planes with surface-charge density M_s separated by an interlayer with thickness L (Fig. 2), the magnetostatic energy is $2\pi M_s^2 f(L)$ where

$$f(L) = \frac{2D}{\pi h}\sum_{k=1}^{\infty}\frac{1-(-1)^k\cos(\pi kq)}{k^3}\exp(-2\pi kL/D). \quad (4)$$

By applying an integral transformation introduced in Ref. 21 Eq. (4) can be written as $f(L)=1-\Omega(L)$ where

$$\Omega(\omega) = \frac{4\omega^2}{\pi hD}\int_0^1 (1-t)\ln\left[1+\frac{\cos^2(\pi q/2)}{\sinh^2(\pi\omega t/D)}\right]dt.$$

Then, the demagnetizing factor $\mathcal{N}$ can be written as

$$\mathcal{N} = 1-\Omega(h)+\Xi_{\Omega}(h,s). \quad (5)$$

The function $1-\Omega(h)$ is the stray-field interaction between the planes within the same Co layers while the energy $\Xi_{\Omega}(h,s)$ describes interlayer interactions. To define this energy we introduce the following auxiliary functions:

$$\Xi_F(h,s) = \sum_{k=1}^{nX-1}\sum_{j=k+1}^{nX}\frac{2F(L_{kj})-F(L_{kj}+h)-F(L_{kj}-h)}{nX} \quad (6)$$

with $L_{kj}=\Sigma_{i=k}^{j-1}[h+s_i]$ and

$$s_i = \begin{cases} 2s+L_b & \text{for } i=mX,\ m=1,\ldots,n \\ t & \text{otherwise.}\end{cases}$$

It should be noted that the sum of functions $2\Omega(L)-\Omega(L+h)-\Omega(L-h)$ equals stray-field coupling energies between two layers separated by distance L between the centers of magnetic layers but Ξ_{Ω} is a sum of all interlayer pairs interactions. In Eq. (6) n is the number of ferromagnetic $[\mathrm{Co/Pt}]_{X-1}/\mathrm{Co}$ subblocks involved in the metamagnetic transition. $n=1$ and $N/2-1$, respectively, for surface and bulk metadomains. The stray-field energy Eq. (5) is the generalization of the energy derived in Refs. 12 and 22, for the case of multilayers with different spacer thicknesses. Such multilayers have, e.g., been treated in Ref. 17.

The equilibrium domain sizes $d_{\pm}$ are derived by minimization of the energy in Eq. (3) with respect to the domain period D and the imbalance of up and down domains q. This leads to the following two coupled implicit equations:

$$\Upsilon(h)-\Xi_{\Upsilon}(h,s) = \pi l_c h,$$

$$\Psi(h)-\Xi_{\Psi}(h,s) = (H-H_{ex})/(2M_s) \quad (7)$$

with

$$\Upsilon(\omega) = \omega^2\int_0^1 t\ln\left[1+\frac{\cos^2(\pi q/2)}{\sinh^2(\pi\omega t/D)}\right]dt$$

and

$$\Psi(\omega) = \frac{\omega^2\sin(\pi q)}{hD}\int_0^1\frac{(1-t)dt}{\sinh^2(\pi\omega t/D)+\cos^2(\pi q/2)}.$$

For the notations of functions Ξ_{Υ} and Ξ_{Ψ} see Eq. (6).

The transition fields $H_{s1,s2}$ delimiting the existence regions for metamagnetic domains equal

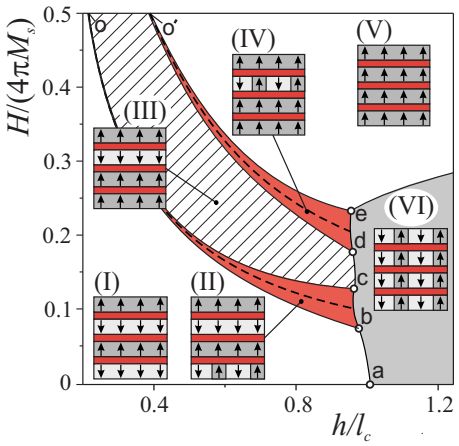

FIG. 3. (Color online) Calculated magnetic-phase diagram for $N=4$, $X=1$, and $J/(2\pi M_s^2)=0.9$ nm introduces possible magnetic phases: (I) antiferromagnetic single-domain state, (II) surface metadomains, (III) ferrimagnetic state, (IV) bulk metadomain, (V) ferromagnetic (saturated) state, and (VI) ferrostripes.

$$H_{s1,s2} = H_{ex} \mp H_s, \quad (8)$$

where the critical field H_s is the transition field of stripe domains for ferromagnetic multilayers, as derived from the equations

$$H_s = M_s[\psi(h)-\Xi_{\psi}(h,s)] \quad (9)$$

and

$$\gamma(h)-\Xi_{\gamma}(h,s) = 2\pi l_c h \quad (10)$$

with

$$\psi(\omega) = 2\omega\,\mathrm{arctg}\left(\frac{\omega}{d_c}\right)-d_c\ln\left[1+\left(\frac{\omega}{d_c}\right)^2\right],$$

$$\gamma(\omega) = d_c^2\ln\left(1+\frac{\omega^2}{d_c^2}\right)+\omega^2\ln\left(1+\frac{d_c^2}{\omega^2}\right).$$

The parameter d_c is equal to the width of the isolated stripe domain of the minority phase at the transition field H_s.[23,24] The functions Ξ_{ψ} and Ξ_{γ} are defined according to Eq. (6).

The typical magnetic-phase diagram of the equilibrium states in reduced variables for layer thickness h/l and applied bias field $H/4\pi M_s$ is shown in Fig. 3. It is calculated for a stack of $N=4$ single ferromagnetic layers ($X=1$) separated by an interlayer with reduced thickness $s/l_c=0.2$, normalized exchange $J/(l_c 2\pi M_s^2)=0.2$, and the assumption of constant characteristic length. This diagram holds six possible magnetic phases labeled as (I)–(VI). At zero field the ferromagnetic stripe domain state (VI) is more favorable for thick layers ($h>h_a$). The antiferromagnetic interlayer coupling causes a relative shift of domains in adjacent layers when forming the ferromagnetic ground state. This leads to an instability of the ferrostripe solutions below the critical thickness h_a, where the homogeneous AF state (I) becomes more favorable.[12] For external fields parallel to the surface normal the transition between homogeneous AF state and the ferrostripes occurs along the line a-b ($h_b<h_a$). Such transitions

have been observed in (Co/Pt)Ru multilayers with wedged Co layers.[6] For $h<h_b$ an increasing magnetic field induces three successive transitions. Critical lines *ob* and *oc* confine the region with surface metamagnetic domains [phase (II)]. At the transition line *o*-*c* the surface layer reaches the saturated state. The system remains in this so-called ferrimagnetic state (III) up to the transition into the bulk (or internal) metamagnetic state (IV) (line *o'*-*d*). The two dashed lines in Fig. 3 are defined by Eq. (2). At these special lines the competing domains have the same sizes, $d^{(+)}=d^{(-)}(q=0)$, and the total magnetization of the multilayer includes contributions only from the saturated layers. In particular, for $N=4$, the total magnetization at these lines equals $(1/4)M_s^*$ (surface domains) and $(3/4)M_s^*$ (bulk domains). $M_s^*=M_sNX$ is defined as the saturation magnetization of a multilayer containing NX cobalt layers. This allows to extract values of the exchange coupling from the magnetization curves. For $N=4$ both the surface and bulk metamagnetic domains are formed only in one layer (Fig. 3). For multilayers with $N>4$ the bulk metamagnetic transition involves more than one layer. Correspondingly, such transitions have wider existence regions than those for surface domains. Thus, for a larger number N of ferromagnetic blocks, the regions with surface and bulk domains merge ($H_d<H_b$). In this case metamagnetic domains occur all along the stack similarly to domains in the ferrostripe phase (VI), however, only every second layer forms the stripes, as the intervening layers are already fully saturated. For these configurations $n=N/2$ and the parameter in the definition of the bias field, Eq. (2), is given by $\alpha=(2n-1)/n$. Accordingly, for $H=H_{ex}$ the magnetization equals $(1/2)M_s^*$.

III. EXPERIMENTS

To test the theoretical results, we have experimentally investigated the ground state and field-driven behavior of $\{[\mathrm{Co}(4\ \text{Å})/\mathrm{Pt}(7\ \text{Å})]_{X-1}/\mathrm{Co}(4\ \text{Å})/\mathrm{Ru}(9\ \text{Å})\}_N$ multilayers with $N=18$ and $X=7$, 8, and 9 and another multilayer with $N=10$ and $X=5$. The sample series with $N=18$ and varying X has been chosen to test the predictions of Fig. 3, which suggest metamagnetic transitions for films with AF ground state (small Co/Pt thickness) and a simple FM behavior for multilayers with larger Co/Pt thickness. Indeed, the zero-field domain structure was found to be ferromagnetic for samples with $X=9$ (Refs. 6 and 17) and antiferromagnetic for multilayers with $X=7$ and 8.[6] The additional prediction of separated bulk and surface metamagnetic transitions is best studied in the multilayer with $N=10$ and $X=5$. The samples were prepared by magnetron sputtering (3 m Torr Ar pressure) at ambient temperature onto Si_3N_x-coated Si substrates with a 20-nm Pt seed layer and a 2-nm Pt cap for oxidation protection. Details on sample preparation are given in Ref. 6.

Magnetic hysteresis at room temperature, with field perpendicular to the film plane was measured using a Quantum Design physical-properties-measurement system with vibrating-sample magnetometer (VSM) in a maximum field of 3 T or a superconducting quantum interference device (SQUID) magnetometer. In one sample ($N=18$, $X=8$) the evolution of the domain structure has been studied via in-field magnetic-force microscopy (MFM). The measurements were performed using a digital instrument Dimension 3100 atomic-force microscope with MFM extender box for phase-shift measurements. The topography scan was conducted in tapping mode and the magnetic contrast was measured in an interleave scan with a lift height of 50 nm. Standard magnetic tips were magnetized along the tip axis prior to the MFM measurements. The MFM measurements in field were performed using a strong pyramid permanent magnet assembly which was lifted gradually to approach the sample from below. The field distribution above the permanent magnet was measured with a Mag-Scan Hall-probe system. The lateral homogeneity is better than 1% within a radius of 2 mm from the center of this permanent magnet.[17]

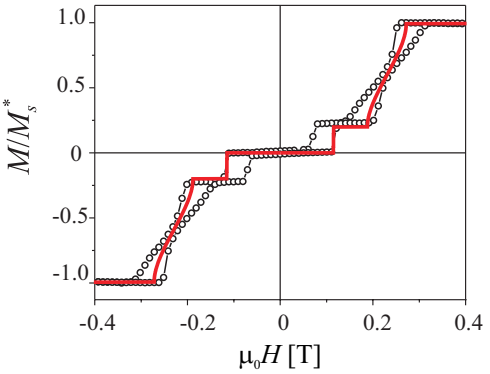

FIG. 4. (Color online) SQUID hysteresis loop measured at for $[\mathrm{Co}(4\ \text{Å})/\mathrm{Pt}(7\ \text{Å})]_{X-1}/\mathrm{Co}(4\ \text{Å})/\mathrm{Ru}(9\ \text{Å})_N$ multilayers with $X=5$ and $N=10$ (open symbols). Solid line correspond to the calculated magnetization curve for equilibrium states.

IV. COMPARISON OF EXPERIMENTAL AND THEORETICAL RESULTS

Figures 4 and 5 show the hysteresis loops of the samples measured at 300 K with the magnetic field applied perpendicular to the sample surface. The magnetization curve for a $\{[\mathrm{Co}(4\ \text{Å})/\mathrm{Pt}(7\ \text{Å})]_4/\mathrm{Co}(4\ \text{Å})/\mathrm{Ru}(9\ \text{Å})\}_{10}$ multilayer with separate surface- and bulk-reversal steps (Fig. 4) clearly demonstrates the two-step character of the metamagnetic transition. The smaller steps at ± 0.12 T result from the switching of the surface blocks at either the top or the bottom of the multilayer stack. The larger reversal steps occurring at higher fields ($H=\pm 0.32$ T) are connected with the bulk metamagnetic transition. Such a distinct two-step reversal is expected for this multilayer since it has a small number of Co/Pt repeats X per block.

Magnetization curves for the samples with $N=18$ (Fig. 5) reveal other possible scenario of metamagnetic transition. For $X=8$, at small magnetic fields up to about 0.2 T, the sample displays a plateau region in which the magnetization of the [Co/Pt] blocks aligns in an AF configuration along the easy axis and is therefore less susceptible to the applied field. Increasing the field value above 0.2 T the antiferromagnetic coupling strength is exceeded which leads to a steplike increase in the magnetization. For higher fields, magnetization

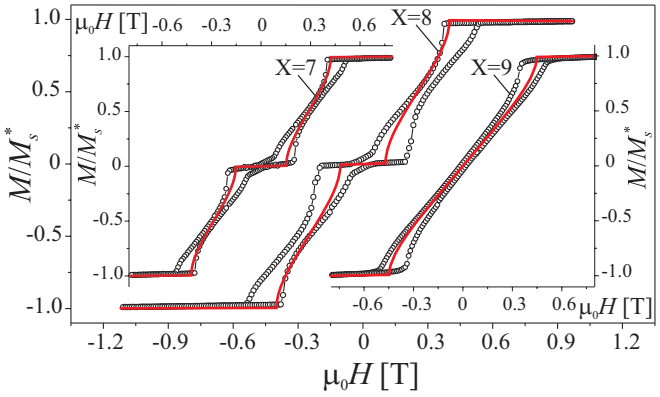

FIG. 5. (Color online) Hysteresis loop for $N=18$ and $X=8$ measured by VSM with the field perpendicular to the sample surface. Insets shows magnetization curves for $X=7$ (Ref. 25) and 9 (Ref. 17). Solid lines correspond to the theoretically calculated magnetization curve of equilibrium states.

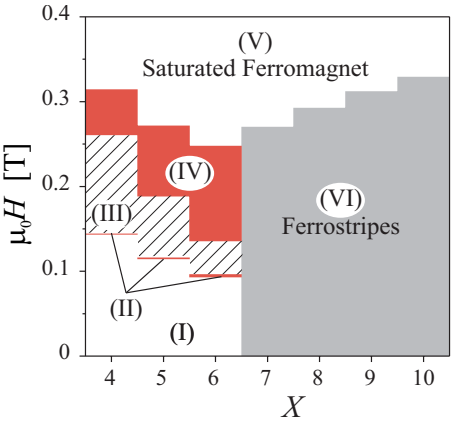

FIG. 6. (Color online) Magnetic-phase diagram with X and a bias field H as independent variables for the [Co/Pt]/Ru multilayer with $N=10$ and $J=0.39$ erg/cm^2. For $X\geq 7$ the system has FM striped ground state. For thin ferroblocks $X\leq 6$ the regions with surface (II) and bulk (IV) metamagnetic domains are separated by the ferrimagnetic phase (III).

increases almost linearly until it reaches saturation. In the field region of 0.2–0.6 T a mixed state of metamagnetic domains is expected which is studied in more detail by in-field MFM observation. A similar behavior has been observed for a multilayer with $X=7$ (Refs. 25 and 26) while for $X=9$, the system shows a purely ferromagnetic behavior,[17] as obvious from the absence of the plateau around remanence.

Strictly speaking the calculation of ground states of the system described with Eq. (3) can be done with reduced control parameters such as $H/(4\pi M_s)$, $J/(2\pi M_s^2)$, h/l_c, t/l_c, s/l_c, N, and X. However to define quantitative properties of the system one should determine the material parameters J, M_s, and l_c in addition to the geometrical parameters.

From the magnetization curves for the samples with $N=10$, $X=5$ (Fig. 4) and $N=18$, $X=7$ (Fig. 5) we estimate the exchange field as the one corresponding to the center between up and down branches at M/M_s^* equal to the middle of magnetization step. Theoretically the middle of magnetization steps corresponding to the bulk ($N=10$, $X=5$) and mixed ($N=18$, $X=7$) metamagnetic transition are equal $M/M_s^*=\frac{3}{5}$ and $=\frac{1}{2}$, respectively. Then in accordance with Eq. (2) we determine the interlayer exchange constants for these systems as $J=0.391$ erg/cm^2 for $N=10$, $X=5$, and 0.73 erg/cm^2 for $N=18$, $X=7$. For $N=10$, $X=5$ we used the magnetization step corresponding to the bulk metamagnetic transition only. This choice is necessitated because of the strong hysteretic effect in surface metamagnetic transition which hampers accurate identification of the exchange field.

From the experimental measurements for the $\{[\text{Co}(4\ \text{Å})/\text{Pt}(7\ \text{Å})]_8/\text{Co}(4\ \text{Å})/\text{Ru}(9\ \text{Å})\}_{18}$ multilayer[17] we estimated saturation magnetization of individual cobalt layer as $M_s=1700$ emu/cm^3. We had estimated the value of $l_c=4.43$ nm as a best fit of the experimentally measured dependence of stripe domain period versus number of cobalt layers X in a pure $[\text{Co}/\text{Pt}]_X$ multilayer.[6,24] The solid lines in Figs. 4 and 5 have been calculated as anhysteretic magnetization curves from Eq. (7) under the assumption that the average magnetization of the multilayer is

$$M=\begin{cases}\frac{1}{2}M_s^*\left[\frac{1}{5}(1+q_s)+\frac{4}{5}(1+q_b)\right], & N=10,\ X=5\\ \frac{1}{2}M_s^*[1+q_m], & N=18,\ X=7\ \text{and}\ 8,\end{cases}$$

where subindexes s, b, and m correspond to the surface, bulk and mixed type of metamagnetic transition, respectively. It can be seen, that the general behavior, i.e., the appearance or absence of bulk and surface metadomains and also the general approach to saturation is well described by the calculations whereas the hysteretic experimental behavior stemming from domain-wall pinning can obviously not be explained by the anhysteretic model.

The phase diagrams Figs. 6 and 7 show existence regions for the magnetic states in the multilayer with fixed number N and different values of X. These diagrams may be regarded as discretized analogs of Fig. 3. The thickness of $[\text{Co}(4\ \text{Å})/\text{Pt}(7\ \text{Å})]_{X-1}/\text{Co}(4\ \text{Å})$ block does not vary continuously but in discrete steps with the number of cobalt layers X. Furthermore we take into account magnetostatic interaction between individual ferromagnetic layers and fix corresponding material parameters of each cobalt layer ($l_c=4.43$ nm and $M_s=1700$ emu/cm^3).

The phase diagrams display how the metamagnetic multidomain states change for the experimentally studied multilayers. As discussed with respect to Fig. 3, for large thickness of the ferromagnetic block, the multilayer remains in the ferrostripe regime (VI) for all applied fields until the sample saturates (V). For the studied systems this behavior is expected for $X\geq 7$ ($N=10$) and $X\geq 9$ ($N=18$). Multilayers with smaller number of layers ($X\leq 6$ for both systems) show a two-step magnetization behavior with a pronounced plateau at $M=0$ for small fields until the surface layer switches through a surface metamagnetic transition in a small field range (II) as visible in Fig. 4 for $N=10$ and $X=5$. This is followed by a second plateau (III) that marks the existence range of the surface metadomains. Then follows the well-

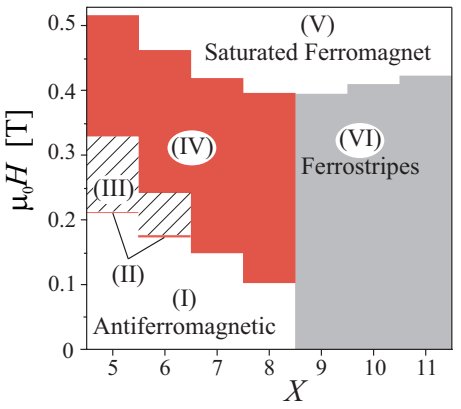

FIG. 7. (Color online) Magnetic-phase diagram with X and a bias field H as independent variables for the [Co/Pt]/Ru multilayer with $N=18$ and $J=0.73$ erg/cm^2. For $X \geq 9$ the system has FM striped ground state. For thin ferroblocks $X \leq 6$ the regions with surface (II) and bulk (IV) metamagnetic domains are separated by the ferrimagnetic phase (III). For $X=7,8$ metamagnetic domains are formed all along the stack.

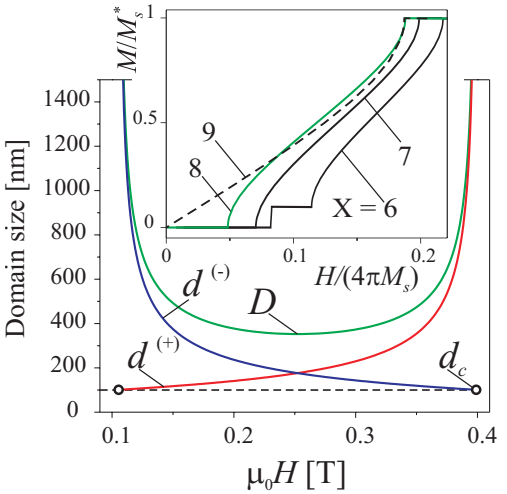

FIG. 8. (Color online) The equilibrium values of domain sizes $d_{\pm}$ and the stripe period D as functions of the applied field in the multilayer with $N=18$, $X=8$. The open circles denote the critical width of isolated stripe domains of minority phase d_c at critical fields H_{s1} and H_{s2}. The inset shows the theoretical magnetization curves for $X=6$, 7, 8, and 9.

separated bulk metamagnetic transition. Here, stripe domains exist alternatingly in internal layers of the multilayer stack, as sketched in Fig. 2(a). For intermediate thickness ($X=7,8$) of $N=18$ surface and bulk metamagnetic transition merge. Thus, only a single-step magnetization process is observed when the field overcomes the AF coupling. In those cases, the surface and internal metamagnetic domain structures take on a mixed appearance. These theoretical results are matched by the hysteresis measurements presented in Fig. 5 and by other experimental findings of Refs. 6 and 17.

The equilibrium metamagnetic stripe domain sizes for the multilayers with $N=18$, $X=8$ are plotted in Fig. 8. While d^+ and d^- grow and shrink at the cost of each other, the domain period develops a minimum at $H=H_{ex}$. Particularly, we find that the smallest domain period, $D=352.6$ nm should be observed for $H=H_{ex}$ at a field of 0.253 T. The isolated stripe domains of the minority phase have the same width $d_c=101$ nm for $H=H_{s1}$ (0.104 T) and $H=H_{s2}$ (0.4 T) (see Fig. 8). The calculated magnetization curves for $N=18$ and different values of X (Fig. 8, inset) reflect the different types of reorientations in the system. The same magnetization curves are plotted in Fig. 5 for comparison with the experimental data.

At the critical field H_{s1} (H_{s2}) the metamagnetic stripes transform into the homogeneous antiferromagnetic phase (saturated ferrimagnet). During this transition the period extends to infinity while the size of the minority phase $d^{(-)}$ has a finite value at the saturating field $H=H_{s2}$ as well as $d^{(+)}$ at $H=H_{s1}$ (Fig. 8).

As it shown in Fig. 9 the behavior of equilibrium domains for bulk and surface metamagnetic transition for multilayers with $N=10$, $X=5$ within the corresponding field limits is the same as for the mixed type of metamagnetic transition (Fig. 8). However, equilibrium domain sizes of the surface metadomains are much larger than for the bulk metadomains and exist only in a much narrower field region. In particular, the critical width of isolated stripe domains of the minority phase by surface metamagnetic transition is $d_c=2.98$ μm. This value is more than twenty times larger than the corresponding value of $d_c=127.45$ nm for bulk metamagnetic domains and more than six hundred times larger than the total thicknesses of the ferromagnetic blocks with $X=5$. The equilibrium domain patterns can hardly be formed in such system. The energy gain in the demagnetized state becomes very small for such thin multilayers and any trace of wall coercivity will suppress the formation of equilibrium domains.[16] That is why the surface transition in the experimental data Fig. 4 is characterized by strongly hysteretic loops compared to the bulk transition.

So far, only homogeneously magnetized blocks or metamagnetic (parallel) stripes have been considered as possible domain configuration. In real multilayers near the transition fields, the regular stripes transform into a system of isolated minority stripes. From the magnetization process in purely ferromagnetic multilayers with perpendicular anisotropy it is known that, close to saturation, the minority domains degenerate into bubbles, which finally collapse. Owing to the close physical relation between the metamagnetic domains and those in ferromagnetic multilayers we can give a more detailed description of the metamagnetic domain evolution in a field by including bubble domain formation, as in Refs. 6 and 17. Thus, the instability of the stripe structure indicates the transformation of minority stripes into isolated bubbles [Fig. 10, insets A and B] Isolated stripes can exist as metastable entities within broad ranges of the magnetic fields (dashed areas in Fig. 10). Metamagnetic bubble domains can exist as isolated entities or they may condense into regular hexagonal lattices. Thus, these domains can also be formed during the metamagnetic transitions. Micromagnetic equations for such domains can be readily derived from the corresponding equations for bubbles in ferromagnetic multilayers.[17] The calculated bubble collapse fields $H_{c1,2}$ and bubble strip-out (elliptic instability) fields $H_{e1,2}$ are marked in Fig. 10. It should be noted that metamagnetic bubble do-

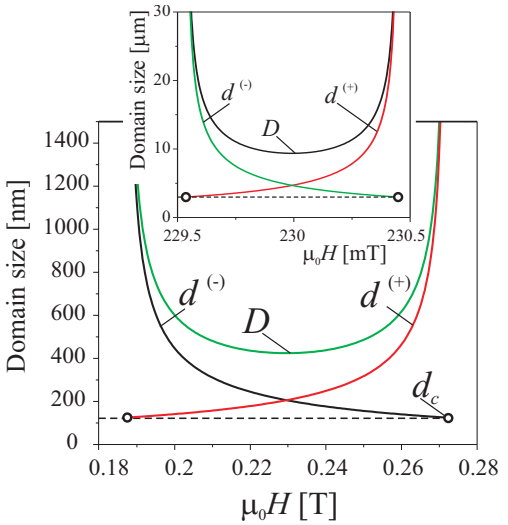

FIG. 9. (Color online) The equilibrium values of domain sizes as functions of the applied field in the multilayer with $N=10$, $X=5$ at bulk metamagnetic transition. The inset shows the equilibrium domain sizes at the surface metamagnetic transition for the same sample. The open circles denote the critical width of isolated stripe domains of minority phase d_c at critical fields H_{s1} and H_{s2} (see Fig. 8).

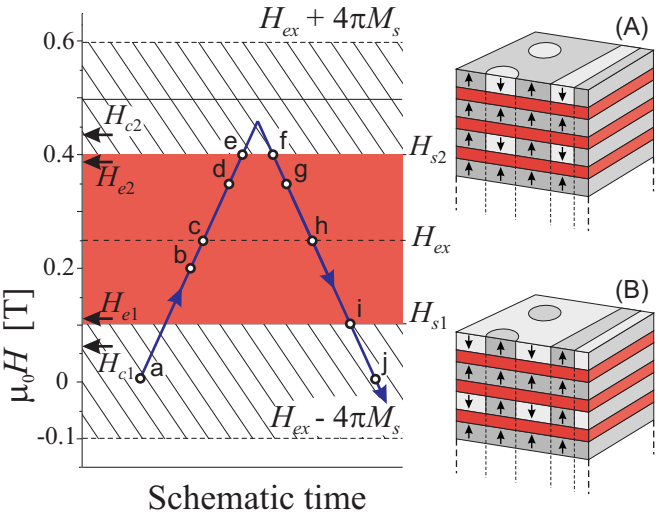

FIG. 10. (Color online) Details of the phase diagram (Fig. 7) for $X=8$. Shaded (red) area indicates the region with metamagnetic domains. At critical fields H_{s1} (H_{s2}) the metamagnetic striped phase transforms into a system of isolated ferromagnetic stripes within the saturated ferromagnetic (antiferromagnetic) state shown in Inset A (B). They can exist as metastable structures within dashed areas. Arrows indicate the critical fields for isolated bubbles. A set of point *a-b-c-d-e-f-g-h-i-j* show a succession of MFM images as presented in Fig. 11.

mains in AF-coupled multilayers have peculiar property. In particular, regular lattices of metamagnetic bubble domains could be stabilized at zero external field, just by tuning the material and/or geometrical parameters of multilayers. In contrast, bubble domain lattices usually cannot be a favored state at zero field in single magnetic layers or in ferromagnetically coupled multilayers.[16]

The MFM images in Fig. 11 show the domain evolution with magnetic field starting from the AF state [Fig. 11(a)]. Applying small fields, the initial AF state is preserved which corresponds to the plateau region of the hysteresis (Fig. 5). At 0.2 T the AF state is overcome. Then ferromagnetic domains with magnetization pointing along the applied field (dark contrast) are formed in those layers with magnetization antiparallel to the field [Fig. 11(b)]. This corresponds to the simultaneous formation of surface and bulk metadomains (IV), as displayed in Fig. 7 for $X=8$. Increasing the magnetic field further, the up-domains with widths $d^{(+)}$ in the metamagnetic stripes grow at the cost of the down domains with width $d^{(-)}$. This process, occurs first by increase in length of finite domain strips while their width stays essentially constant (not shown here). At an applied magnetic bias field of about 0.25 T [Fig. 11(c)] the metamagnetic up- and down-domains adopt an almost balanced configuration with a domain period $D \approx 500$ nm, as compared with the expected value of 353 nm. The theoretical estimate is in reasonable agreement with observations. Still, the deviation between the

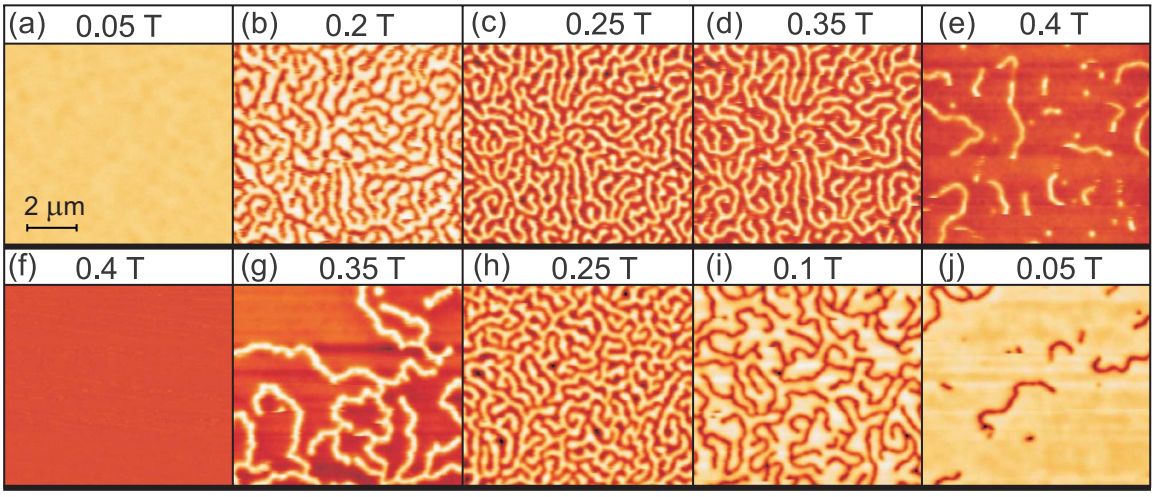

FIG. 11. (Color online) Domain structures of $[\mathrm{Co}(4\ \text{Å})/\mathrm{Pt}(7\ \text{Å})]_{X-1}/\mathrm{Co}(4\ \text{Å})/\mathrm{Ru}(9\ \text{Å})_N$ multilayers with $X=8$ and $N=18$ measured by MFM in a magnetic field.

experiment and the theoretical result for the domain period is significant. The discrepancy may be explained by (i) roughness effects and hysteretic behavior of the system (in the same way as pinning will lead to hysteresis in a field cycle, it may trap domain walls in nonequilibrium position, whereby avoiding the adjustment of equilibrium domain width) and (ii) the fact that we use average values for material parameters, such as J, M_s, and l_c. These parameters fit the system, in general, but could be slightly different in different samples and may result in some deviations of the estimates for domain sizes. Increasing the field further, the minority domains reduce in length [Fig. 11(d)] and finally transform into isolated stripes and bubbles [Fig. 11(e)] at around 0.4 T in very good agreement with the critical field $H_{s,2}$ plotted in Fig. 10. At an applied field of 0.45 T all minority domains have vanished and the sample is fully saturated. Reducing the field leaves the sample in the saturated state at 0.4 T [Fig. 11(f)], which is another manifestation of the hysteresis. Bubble nucleation and strip-out occurs between 0.40 and 0.35 T [Fig. 11(g)] and upon decreasing the field further the bright domains (AF state) increase in length and width until the up domain become isolated and shrink [Figs. 11(h) and 11(i)]. At lowest field, these isolated minority domains vanish almost completely, leaving the multilayer in the original homogeneous AF state. In the MFM observations in Fig. 11 the surface and bulk metamagnetic transition remain coupled in accordance with the phase diagram in Fig. 7. In fact, the surface metamagnetic transition region in the case of $N=10$ as well as for $N=18$ is always very narrow compared to the bulk transition. Moreover, the estimated stripe domain period in the case of surface transition is extremely large. Thus, in real multilayers the nucleation of such multidomain states is hindered and the system exhibits a hysteretic behavior with a square magnetization loop. This explains the data for $N=10$ and $X=5$ in Fig. 4, where the magnetization curve shows a pronounced hysteretic behavior between about 0.1 and 0.2 T, and a second well separated hysteretic reversal above about 0.24 T.

V. CONCLUSIONS

In this paper, we have presented theoretical and experimental investigations of antiferromagnetically coupled multilayer $\{[\mathrm{Co}(4\ \text{Å})/\mathrm{Pt}(7\ \text{Å})]_X/\mathrm{Co}(4\ \text{Å})/\mathrm{Ru}(9\ \text{Å})\}_N$ with a homogeneous AF ground state. Our findings, presented here as well as in previous contributions,[12,13,17] reveal a large variety of possible multidomain states in AF-coupled multilayers with perpendicular anisotropy. The complex evolution of the specific (metamagnetic) multidomain states induced by external fields elucidates reorientation effects and the formation of isolated stripe and bubble domains within the saturated states and antiferromagnetic remanent state.[13,27] Direct observation of metamagnetic domains confirms the theoretical description of this evolution. Within the micromagnetic approach introduced in Ref. 17 metamagnetic domains can be described by a modified model of ferromagnetic domains, Eq. (3) and Fig. 2. This allows to derive the equilibrium parameters of metamagnetic stripe and bubble domains and calculate magnetic phase diagrams (Figs. 3, 6, and 7). These diagrams for the field-driven equilibrium states can also provide the basis for future investigations of the hysteretic processes induced by coercivity and the dynamics at the various magnetic phase transitions in these multilayer systems.

ACKNOWLEDGMENTS

The authors thank I. Mönch for a discussion of the experiment. Support by DFG under Grant No. SPP 1239 project A8 is gratefully acknowledged.

*Corresponding author; m.kyselov@ifw-dresden.de
†u.roessler@ifw-dresden.de

[1] E. E. Fullerton, D. T. Margulies, N. Supper, Do Hoa, M. Schabes, A. Berger, and A. Moser, IEEE Trans. Magn. **39**, 639 (2003).
[2] L. Trallori, P. Politi, A. Rettori, M. G. Pini, and J. Villain, Phys. Rev. Lett. **72**, 1925 (1994); A. N. Bogdanov and U. K. Rößler, Phys. Rev. B **68**, 012407 (2003); U. K. Rößler and A. N. Bogdanov, *ibid.* **69**, 184420 (2004).
[3] R. W. Wang, D. L. Mills, E. E. Fullerton, J. E. Mattson, and S. D. Bader, Phys. Rev. Lett. **72**, 920 (1994); S. G. E. te Velthuis, J. S. Jiang, S. D. Bader, and G. P. Felcher, *ibid.* **89**, 127203 (2002); V. Lauter-Pasyuk, H. J. Lauter, B. P. Toperverg, L. Romashev, and V. Ustinov, *ibid.* **89**, 167203 (2002).
[4] U. K. Rößler and A. N. Bogdanov, Phys. Rev. B **69**, 094405 (2004); J. Alloys Compd. **423**, 153 (2006).
[5] D. L. Mills, Phys. Rev. Lett. **20**, 18 (1968); F. Keffer and H. Chow, *ibid.* **31**, 1061 (1973).
[6] O. Hellwig, A. Berger, J. B. Kortright, and E. E. Fullerton, J. Magn. Magn. Mater. **319**, 13 (2007).
[7] T. Hauet, C. M. Günther, O. Hovorka, A. Berger, M.-Y. Im, P. Fischer, T. Eimüller, and O. Hellwig, Appl. Phys. Lett. **93**, 042505 (2008).
[8] A. Baruth, L. Yuan, J. D. Burton, K. Janicka, E. Y. Tsymbal, S. H. Liou, and S. Adenwalla, Appl. Phys. Lett. **89**, 202505 (2006).
[9] Z. Y. Liu, N. Li, F. Zhang, B. Xu, J. L. He, D. L. Yu, Y. J. Tian, and G. H. Yu, Appl. Phys. Lett. **93**, 032502 (2008).
[10] Y. Fu, W. Pei, J. Yuan, T. Wang, T. Hasegawa, T. Washiya, H. Saito, and S. Ishio, Appl. Phys. Lett. **91**, 152505 (2007).
[11] J. E. Davies, O. Hellwig, E. E. Fullerton, and K. Liu, Phys. Rev. B **77**, 014421 (2008).
[12] N. S. Kiselev, I. E. Dragunov, U. K. Rößler, and A. N. Bogdanov, Appl. Phys. Lett. **91**, 132507 (2007).
[13] N. S. Kiselev, U. K. Rößler, A. N. Bogdanov, and O. Hellwig, Appl. Phys. Lett. **93**, 162502 (2008).
[14] O. Hellwig, T. L. Kirk, J. B. Kortright, A. Berger, and E. E. Fullerton, Nature Mater. **2**, 112 (2003).
[15] Theory predicts a multidomain state with antiferromagnetic arrangement of domains in adjacent layers as the third possible ground state in multilayers with strong AF exchange (Ref. 12). This phase has not been observed experimentally so far.

[16] A. Hubert and R. Schäfer, *Magnetic Domains* (Springer-Verlag, Berlin, 1998).
[17] C. Bran, A. B. Butenko, N. S. Kiselev, U. Wolff, L. Schultz, O. Hellwig, U. K. Rößler, A. N. Bogdanov, and V. Neu, Phys. Rev. B **79**, 024430 (2009).
[18] E. Stryjewski and N. Giordano, Adv. Phys. **26**, 487 (1977).
[19] U. K. Rößler and A. N. Bogdanov, J. Magn. Magn. Mater. **269**, L287 (2004).
[20] J. F. Dillon, Jr., E. Yi Chen, N. Giordano, and W. P. Wolf, Phys. Rev. Lett. **33**, 98 (1974); E. Y. Chen, J. F. Dillon, and J. H. Guggenheim, J. Appl. Phys. **48**, 804 (1977); O. Petracic, Ch. Binek, and W. Kleemann, *ibid.* **81**, 4145 (1997).
[21] A. N. Bogdanov and D. A. Yablonskii, Fiz. Tverd. Tela (Leningrad) **22**, 680 (1980) [Sov. Phys. Solid State **22**, 399 (1980)].
[22] H. J. G. Draaisma and W. J. M. de Jonge, J. Appl. Phys. **62**, 3318 (1987).
[23] C. Kooy and U. Enz, Philips Res. Rep. **15**, 7 (1960).
[24] N. S. Kiselev, I. E. Dragunov, U. K. Rößler, and A. N. Bogdanov, Pis'ma Zh. Tekh. Fiz. **33** (23), 87 (2007) [Tech. Phys. Lett. **33**, 1028 (2007)].
[25] O. Hellwig, A. Berger, and E. E. Fullerton, Phys. Rev. B **75**, 134416 (2007).
[26] O. Hellwig, A. Berger, and E. E. Fullerton, Phys. Rev. Lett. **91**, 197203 (2003).
[27] N. S. Kiselev, U. K. Rößler, A. N. Bogdanov, and O. Hellwig, J. Magn. Magn. Mater., doi:10.1016/j.jmmm.2009.03.031 (2009).